

Influence of Surface Chemistry on Adhesion and Osteo/Odontogenic Differentiation of Dental Pulp Stem Cells

Ting-Ting Yu,[†] Fu-Zhai Cui,[‡] Qing-Yuan Meng,[‡] Juan Wang,^{§,⊥} De-Cheng Wu,^{§,⊥} Jin Zhang,^{||} Xiao-Xing Kou,[†] Rui-Li Yang,[†] Yan Liu,[†] Yu Shrike Zhang,^{*,||} Fei Yang,^{*,§,⊥} and Yan-Heng Zhou^{*,†}

[†]Center for Craniofacial Stem Cell Research and Regeneration, Department of Orthodontics, Peking University School and Hospital of Stomatology, Beijing 100081, P. R. China

[‡]School of Materials Science and Engineering, Tsinghua University, Beijing 100084, P. R. China

[§]Beijing National Laboratory for Molecular Sciences, State Key Laboratory of Polymer Physics & Chemistry, Institute of Chemistry, Chinese Academy of Sciences, Beijing 100190, P. R. China

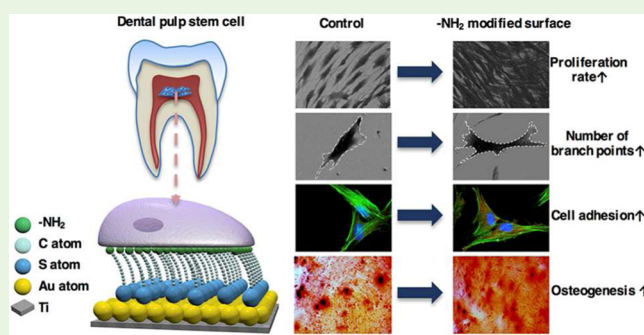
[⊥]University of Chinese Academy of Sciences, Beijing 100049, P. R. China

^{||}Division of Engineering in Medicine, Department of Medicine, Brigham and Women's Hospital, Harvard Medical School, Cambridge, Massachusetts 02139, United States

Supporting Information

ABSTRACT: The complex interaction between extracellular matrix and cells makes the design of materials for dental regeneration challenging. Chemical composition is an important characteristic of biomaterial surfaces, which plays an essential role in modulating the adhesion and function of cells. The effect of different chemical groups on directing the fate of human dental pulp stem cells (hDPSCs) was thus explored in our study. A range of self-assembled monolayers (SAMs) with amino ($-\text{NH}_2$), hydroxyl ($-\text{OH}$), carboxyl ($-\text{COOH}$), and methyl ($-\text{CH}_3$) modifications were prepared. Proliferation, morphology, adhesion, and differentiation of hDPSCs were then analyzed to demonstrate the effects of surface chemical groups. The results showed that hDPSCs attached to the $-\text{NH}_2$ surface displayed a highly branched osteocyte-like morphology with improved cell adhesion and proliferation abilities. Moreover, hDPSCs cultured on the $-\text{NH}_2$ surface also tended to obtain an increased osteo/odontogenesis differentiation potential. However, the hDPSCs on the $-\text{COOH}$, $-\text{OH}$, and $-\text{CH}_3$ surfaces preferred to maintain the mesenchymal stem cell-like phenotype. In summary, this study indicated the influence of chemical groups on hDPSCs in vitro and demonstrated that $-\text{NH}_2$ might be a promising surface modification strategy to achieve improved biocompatibility, osteoconductivity/osteoinductivity, and osseointegration of dental implants, potentially facilitating dental tissue regeneration.

KEYWORDS: surface chemistry, dental pulp stem cells, adhesion, cell fate, self-assembled monolayer



1. INTRODUCTION

For many years, titanium (Ti) and its alloys have been the most commonly used material in dental and orthopedic implants, based on its appropriate mechanical strength and intrinsic ability to support osseointegration.¹ However, the osseointegration process usually takes long,² and more often, a thin amorphous zone or lamina limitan will appear between the bone and the implant surface.³ These challenges lead to increased risks of implant failure in clinic.^{4,5} To achieve a faster and enhanced osseointegration ability, more bioactive Ti surfaces are needed. Inspired by the natural biomineralization process, more recent research has focused on surface modification methods that can possibly simulate this process to accelerate bone formation on implant surfaces. Li et al. found that the sol-gel-prepared Ti may nucleate Ca/P due to the abundant $-\text{OH}$ groups on the surface.⁶ Campbell et al.

introduced $-\text{SO}_3\text{H}$ to the surface of Ti to initiate Ca/P deposition.⁷ These studies indicated that a proper chemical composition is essential in the biomineralization process to facilitate bone formation.

Many studies have further investigated the interactions between cells and material surfaces, and have revealed the importance of chemical functional groups and how their associated difference in hydrophilicity could have affected cell shape, adhesion, and differentiation.^{8–13} It is known that the differential cell shape¹⁴ and adhesion¹⁵ caused by the properties of the material surfaces can modulate the stem cells fate, potentially through the alteration of downstream signaling

Received: May 2, 2017

Accepted: May 8, 2017

Published: May 8, 2017

pathways that direct cell proliferation, and differentiation.¹³ Rowena et al. indicated that human bone marrow mesenchymal stem cells (hBMMSCs) needed to spread, adhere, and flatten to undergo efficient osteogenesis, while nonspreading, rounded cells mostly became adipocytes.¹⁶ Furthermore, several studies demonstrated the influence of surface chemistry on cellular responses.^{13,17,18} For example, Allen et al. showed different gene expression profiles in cells on surfaces of varying hydrophobicity.¹⁷ These studies indicated that the chemical structure on the surface may guide stem cell fate on-demand, but the research on dental stem cells is still rare. Currently, there have rarely been investigations on the effect of surface chemical modification on dental stem cells, especially its role on directing cells toward the odonto/osteogenic lineage under the stimuli of different surface chemistries.

Moreover, teeth constitute a promising cell source that can be used for a range of therapeutic and regenerative medicine applications.¹⁹ Dental pulp stem cells (DPSCs) are of particular interest among all the dental stem cells, since they are convenient and affordable to collect from extracted third molars or orthodontically extracted teeth in dental clinics. DPSCs originate from migrating neural crest cells and have multipotent differentiation ability, such as osteogenesis, chondrogenesis, adipogenesis, odontogenesis, and neurogenesis, under appropriate inductive conditions.^{20–22} Alge et al. investigated the difference between DPSCs and BMMSCs, and verified that DPSCs obtained an elevated clonogenic ability, an increased proliferation rate, and a higher mineralization potential compared to BMMSC.²² In vivo studies also proved that DPSCs represented an excellent cell source to regenerate bone defect in large animals.^{23–25} Indeed, using DPSCs it was capable of producing new woven bones, so as to accelerate the implant loading time.²⁶ These advantages suggested that DPSCs are a promising cell source for applications in dental regeneration.

A key challenge in stem cell research is to direct their differentiation toward specific lineages in a well-controlled manner. Notably, materials with various characteristics have been generated and applied for dental and bone regeneration protocols with dental stem cells.^{27–31} Recent studies have demonstrated that demineralized/chemically treated dentin matrices (TDM)²⁷ or cryopreserved TDM (CTDM) with proper mechanical and biological characteristics,²⁸ could promote the adhesion of DPSCs and guide the cells into dentinogenic differentiation.²⁹ We previously studied the interplay between intrafibrillarly mineralized collagen (IMC) and dental stem cells, and found that the surface chemical structure could contribute to directing the cells toward osteogenic differentiation.³²

Based on the promising effect of surface chemical modification, more systematic investigations have been performed in this study, focusing on the surface chemical groups and their roles on regulating the proliferation, adhesion, morphology, and osteo/odontogenic differentiation of human DPSCs (hDPSCs). Self-assembled monolayers (SAMs) as a surface modification method, which can achieve a stable, reproducible, and patterned chemical surfaces,^{33–36} have been widely utilized to investigate biomineralization processes^{34,35} and cell behaviors.^{10–13,36,37} Among all, amino ($-\text{NH}_2$), hydroxyl ($-\text{OH}$), carboxyl ($-\text{COOH}$), and methyl ($-\text{CH}_3$) functional groups have been commonly studied for their effects on stem cell behaviors,^{10–13,36} because all these functional groups naturally occur within the biological system and

represent distinctive physical and chemical characteristics. Therefore, we used SAMs of alkanethiols to prepare a range of chemically defined gold (Au)-coated Ti surfaces with respective functional groups. The hDPSCs were cultured on the surfaces for different time periods, and the influence of chemical groups on hDPSCs was characterized.

2. MATERIALS AND METHODS

2.1. Preparation and Characterization of SAMs on Au-Coated Ti Surfaces. To obtain surfaces with well-defined chemical structures, we used SAMs of alkanethiols on Au. The sequential deposition of Ti (10 nm) and Au (40 nm) films was conducted by electron beam evaporator (ANELVA L-400EK, Canon Anelva Co., Kanagawa, Japan) to obtain Au-coated silicon wafers. 11-amino-1-undecanethiol [$\text{HS}-(\text{CH}_2)_{11}-\text{NH}_2$], 11-mercapto-1-undecanol [$\text{HS}-(\text{CH}_2)_{11}-\text{OH}$], 11-mercaptoundecanoic acid [$\text{HS}-(\text{CH}_2)_{11}-\text{COOH}$], and 1-undecanethiol [$\text{HS}-(\text{CH}_2)_{11}-\text{CH}_3$] were purchased from Sigma-Aldrich (St. Louis, USA). Different chemical groups were grown on Au-deposited films after immersion in 1.0 mmol/L alkanethiol solutions protected from light for overnight at 4 °C. After washing with sterile phosphate-buffered solution (PBS, ThermoFisher, Waltham, USA) and dried using nitrogen (N_2) gas, all coverslips were immersed in 70% (V/V) alcohol overnight. Following the modification, the thickness of the modified chemical layers would be around 2 nm according to its atomic composition and structure patterned on the substrates.^{34,35} We used the Au-only surfaces as the control group.

The surface roughness and topography of each sample was measured using scanning electron microscopy (SEM; Hitachi S-4800, Hitachi, Japan) and atomic force microscopy (AFM; MFP-3D, Asylum Research Inc., Santa Barbara, USA) under contact model. After the modification, each SAM with modified chemical functional groups was characterized by contact angle measurements (DataPhysics, Filderstadt, Germany). Furthermore, ESCALab220i-XL electron spectrometer from VG Scientific was used for X-ray photoelectron spectroscopy (XPS) detection under 300-W Al K α radiation. The base pressure was 3×10^{-9} mbar. C 1s line at 284.8 eV from adventitious carbon was referenced as binding energy. Data analysis was carried out using XPSPEAK.

2.2. Cell Culture. The hDPSCs were obtained from healthy human teeth, which were extracted for orthodontic or impaction reasons from patients of 10–25 years old at Peking University School of Stomatology, under the Ethical Guidelines PKUSSIRB-201311103. For dental pulp retrieval, each tooth was cracked open longitudinally using a bone cutter in a tissue culture hood. Collected pulp tissue was rinsed with PBS, minced into small pieces, and incubated in medium containing 0.25% (W/V) type I collagenase for 30 min and transferred to culture plate filled with culture medium, containing 10% (V/V) fetal bovine serum (FBS, ThermoFisher), 1% (W/V) glutamin (ThermoFisher), and 1% (W/V) streptomycin and penicillin antibiotics (ThermoFisher). The hDPSCs at passage 3 were used in all experiments. To validate the isolated hDPSCs, we assessed the multidifferentiation potential of the cells toward osteogenesis and adipogenesis. In addition, the mesenchymal stem cell (MSC) markers of CD44 and CD90 were tested positive for our isolated hDPSCs, and the hematopoietic lineage markers, such as CD45 and CD34 (Figure S1) were tested negative, by using Accuri C6 flow cytometer (BD Biosciences, San Jose, USA).²⁰

2.3. Cell Viability Assays. Cholecystokinin octapeptide (CCK-8) cell viability assay (Dojindo, Mashikimachi, Japan) was used to examine the cell viability following the manufacturer's protocol. Briefly, the initial density of seeding cells in 96-well plates was 1.0×10^4 cells/well. After hDPSCs were cultured for 1, 3, and 7 days, 300.0 μL of culture medium containing 30.0 μL of CCK-8 was used to incubate with cells for 2 h. Finally, the cell viability was measured using microplate reader under the wavelength at 450 nm (Bio-Rad, Hercules, USA).

2.4. SEM Morphological Observation. To evaluate the influence of chemical group substrata on cells morphology, 1.0×10^4 cells were

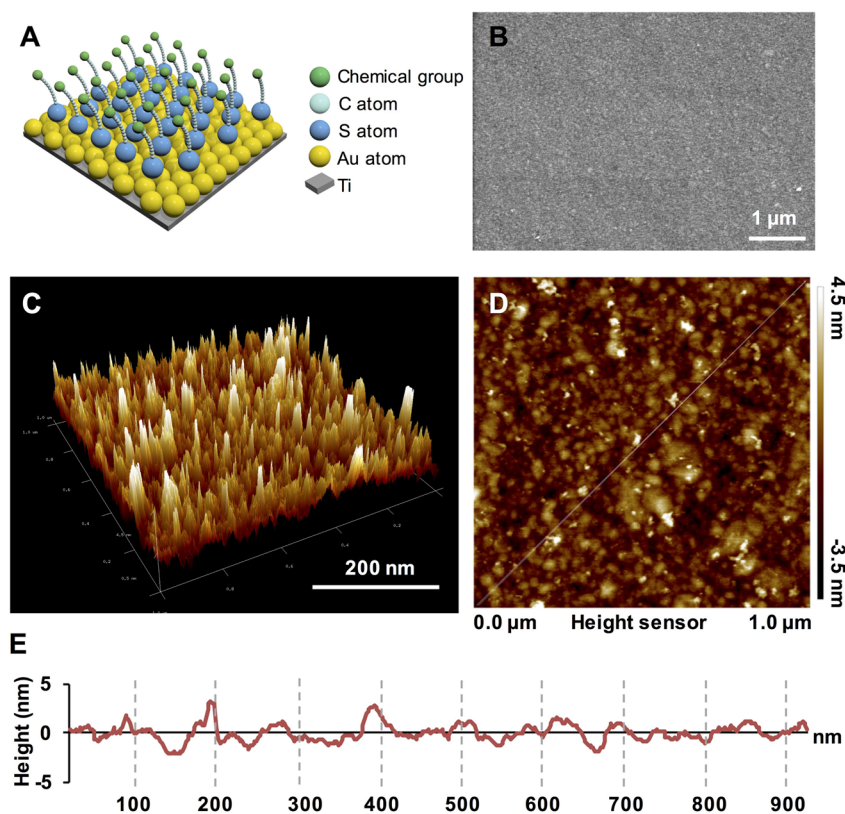


Figure 1. Surface characterization of SAM-modified Au surfaces. (A) Schematic of a thiol monolayer self-assembled on an atomically flat Au-coated Ti substrate; flat Au substrate was observed by (B) SEM and (C–E) AFM. (C) 3D AFM images of the flat Au substrate. (D) Cross-sectional height of flat Au substrate with (E) measurement.

seeded per well. Cell morphology was investigated by SEM at 15 kV. After 1 and 7 days of incubation, nonattached cells on the substrates were removed by washing twice with PBS. Subsequently, 4% (W/V) paraformaldehyde (PFA) was used to fix cells and the samples were thoroughly rinsed with PBS. Afterward, the cells were gradually dehydrated (50, 60, 70, 80, and 90% (V/V) ethanol, each for 15 min) and air-dried for 3 h. At the end, they were sputter-coated with Au (99.99%) and observed by SEM. It is well-established that there is a strong link between cell morphology and cell function.^{32,38,39} While the shapes of the osteoblasts are cuboidal, osteocytes are highly branched. To extract cell morphologies influenced by different chemical groups, we drew cell outlines for branching analysis. Terms used in this study for evaluate branching are defined as follows: the basal dendrites descending from the base of the soma is determined as primary branching point; the dendrites descending from the primary branching are termed secondary branching point; and the dendrites descending from the secondary branching are named tertiary branching points.³⁸ For each group, 50 cells were analyzed. The measurements of cell areas were taken using the ImageJ software (National Institutes of Health, Bethesda, USA). The number of branching points originating from projection with a length of greater than 5 μm^{32,38} was calculated as the number of branching points for each cell.

2.5. Immunofluorescence Assay of Cytoskeleton and Cell Adhesion. 1.0×10^4 cells were seeded and cultivated for 24 h. After fixation, the cells were permeabilized and 10 μg/mL antivinculin antibody (1:500, Sigma-Aldrich) was incubated for overnight at 4 °C. Then Alexa Fluor-647 goat antimouse IgG (1:200, Abcam, Cambridge, USA) and Alexa Fluor 488-Phalloidin (Sigma-Aldrich, St. Louis, USA) at 2 μg/mL were applied. Finally, the mounting medium containing DAPI (Sigma-Aldrich, St. Louis, USA) was used for nuclei staining. To obtain confocal images, the Zeiss laser scanning microscope LSM 510 and LSM 5 Release 4.2 software (Carl Zeiss, Thornwoody, USA) were used.

2.6. Alkaline Phosphatase (ALP) Activity Assay. The hDPPCs were cultured on 24-well plates (1.0×10^5 cells/well) with the culture medium for 7 days. ALP Yellow Liquid substrate system for ELISA (Sigma-Aldrich) was used to analyze the ALP activity on day 7 following the manufacturer's protocol. The values were measured using a microplate reader under a wavelength of 405 nm.

2.7. Osteo/Odontogenic-Related Gene Marker Examination by Polymerase Chain Reaction (PCR). Total RNA was isolated using Trizol reagent (ThermoFisher). Reverse transcription and real-time PCR were followed as previously described.⁴⁰ Expression levels of osteo/odontogenic-related gene markers including Runx2, ALP, DMP-1, and DSPP were quantified, as well as the GAPDH, which served as the housekeeping gene. The primers were commercially synthesized with the sequences indicated below: for human GAPDH, sense 5'-ATGGGAAGGTGAAGGTCG-3', antisense 5'-GGGGTCAT TGATGGCAACAATA-3'; for human Runx2, sense 5'-CCGCCTCAGTGATTTAGGGC-3', antisense 5'-GGGTCTGTAATCTGACTCTGTCC-3'; for human ALP, sense 5'-AACATCAGGGACAT TGACGTG-3', antisense 5'-GTATCTCGTTTGAAGCTCTTCC-3'; for human DMP-1, sense 5'-TGGCGATGCAGGTCACAAT-3', antisense 5'-CCATTCCCAC-TAGGACTCCCA-3'; for human DSPP, sense 5'-AGGAAGTCTGC-CATCTCAGAG-3', antisense 5'-TGGAGTTGCTGTTTTCTGTA-GAG-3'; The melting curve was used to determine the efficiency of the primers.

2.8. Western Blot Analysis. Proteins were obtained using the M-PER mammalian protein extraction reagent (ThermoFisher). A 4–12% NuPAGE gel (ThermoFisher) was used to separate the applied proteins, which were then transferred to 0.2-μm nitrocellulose membranes (Millipore, Billerica, USA). After blocking for 1 h, primary antibodies were applied to incubate the membranes for overnight at 4 °C. Afterward, the membranes were thoroughly washed and incubated in HRP-conjugated IgG (Santa Cruz Biotechnologies, Dallas, USA; 1:10,000) for 1 h. SuperSignal West Pico Chemiluminescent Substrate

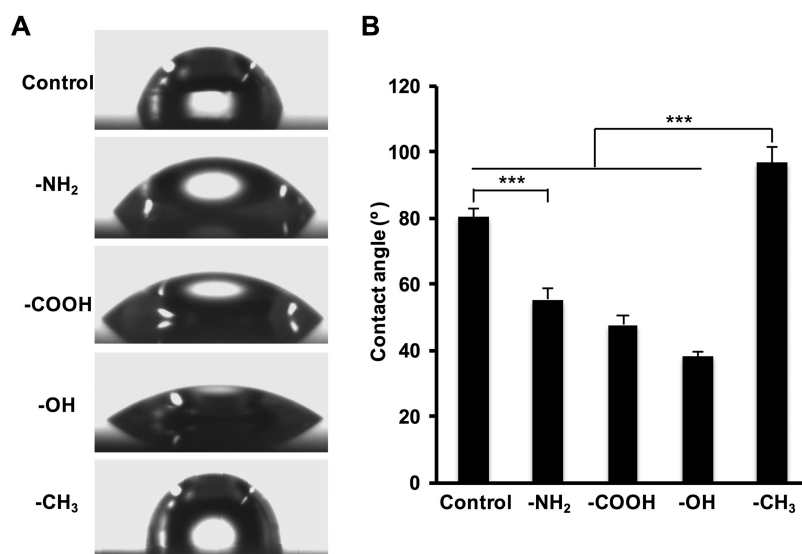


Figure 2. Contact angles of SAM-modified surfaces. Shown are (A) droplet profiles and (B) contact angle measurements. Five droplets were analyzed with contact angles measured from both sides. *** $P < 0.001$.

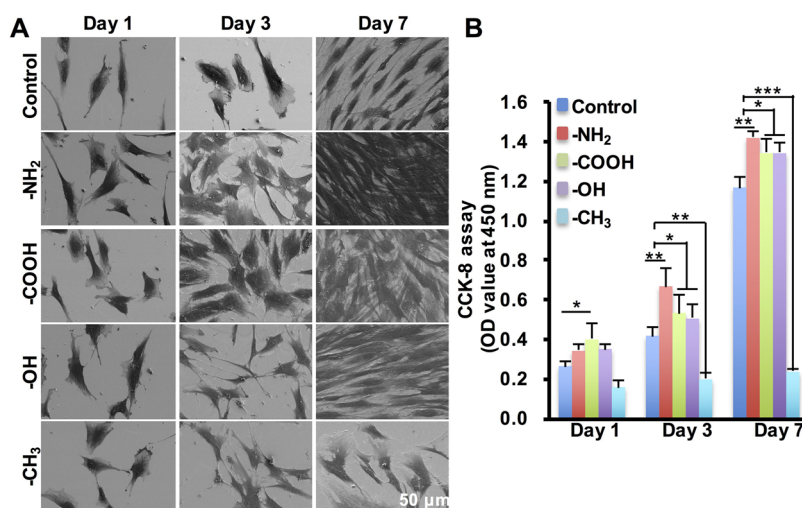


Figure 3. Cell proliferation characterization via (A) SEM and (B) CCK-8 assay of hDPSCs on surfaces functionalized with different chemical groups after 1, 3, and 7 days of incubation. Scale bar = 50 μm . * $P < 0.05$, ** $P < 0.01$, *** $P < 0.001$.

(ThermoFisher) and BioMax film (Kodak, Rochester, USA) were used to detect immunoreactive proteins. β -actin antibody was used to quantify the protein loading amount. We purchased Anti- β -actin antibody from Sigma-Aldrich, while ALP, Runx2, DSPP, and DMP-1 antibodies were obtained from Santa Cruz Biotechnology (Santa Cruz Biotechnologies).

2.9. Alizarin Red S (ARS) Staining. The hDPSCs were cultured under osteogenic conditions (1×10^{-7} M dexamethasone, 10 mM β -glycerophosphate, and 0.05 mM L-ascorbic acid phosphates in the culture medium). After 3 weeks of differentiation, the cells were fixed using 4% PFA. Matrix mineralization was stained by 2% ARS staining and the samples were measured for mineralized nodule formation.

2.10. Data Analysis. SPSS 13.0 program (SPSS Inc. Chicago, Illinois, USA) was used to perform statistical analysis. All data were presented as mean \pm standard deviation. Comparisons between groups were assessed using one-way ANOVA. Values of $P < 0.05$ were considered statistically significant.

3. RESULTS

3.1. Physicochemical Characterization of Different Surfaces.

The topography and roughness of SAM formation

on Au-coated surfaces were observed by SEM (Figure 1B) and AFM (Figures 1C–E). The images proved the smoothness of the surfaces. The results of water dynamic contact angle measurements for SAM-modified surface are shown in Figure 2. Among all the experimental groups, the $-\text{OH}$ surface appeared to be the most hydrophilic one ($38.2 \pm 1.3^\circ$), whereas the $-\text{CH}_3$ surface was the most hydrophobic ($96.8 \pm 4.5^\circ$) due to its nonpolar characteristics. Moreover, the contact angle of the $-\text{NH}_2$ surface was $55.5 \pm 3.4^\circ$, higher than that for the $-\text{COOH}$ surface ($47.7 \pm 2.9^\circ$), although both could still be classified as hydrophilic. The surface wettability values we obtained here are consistent with the literature.^{10–12,34–36} Furthermore, the atomic compositions of the surfaces were analyzed by XPS (Figure S1, Tables S1 and S2). The introduction of mercapto ligand to the Au-coated Ti surface was demonstrated by the decrease in the Au content and increase in the S content. The detection of 2.7% N element further confirmed that the surface was successfully modified with amine groups. The functional compositions of the surfaces were determined from the C 1s core levels. Figure S1 shows the

peaks of C 1s on the surface of the Ti–Au plate modified by the four groups, and the results were consistent with the corresponding chemical structures. The appearance of the C–N peak (Figure S1A), the O=C=O peak (Figure S1B), and the C–O peak (Figure S1C) showed that the –NH₂, –COOH, and –OH groups were introduced to the surfaces, respectively. In comparison, there was only the C–C peak appearing in Figure S1D, consistent with the surface modified with the –CH₃ group. Meanwhile, based on the calculation of S and Au atomic compositions, the comparable S/Au ratios at around 0.11 verified that all the modified surfaces had similar densities of the functional groups. Other information related with these surfaces such as AFM and Fourier transform infrared spectroscopy (FTIR) have been reported in our previous studies.^{34–36}

3.2. Cell Viability Related to Different Chemical Groups. The effects of surface-modified substrates on the proliferative activity of hDPSCs were assessed by SEM and CCK-8 analyses. Figure 3A shows the SEM images, which represented the distinct cell densities after hDPSCs were cultured on different chemically modified surfaces on days 1, 3, and 7. These results were further supported by CCK-8 analysis of hDPSCs at the same time points (Figure 3B). On day 1, –OH, –NH₂, and –CH₃ surfaces displayed similar cell viability with the control group, whereas the level of cell viability on the –COOH substrates was significantly elevated compared with the control group. By days 3 and 7, the values of viable cells on all different substrates had significantly increased with the cell growth on the –CH₃ surface. On days 1, 3, and 7, the least amount of viable cells was found on the –CH₃ surface, especially on days 3 and 7, where the values were significantly lower than all other surfaces. On days 3 and 7, however, a significant increase in the number of viable cells was detected on the –NH₂ surface, and the value was significant higher than all other modified surfaces at the same days. However, the –COOH and OH surfaces also supported cell growth, and their 3- and 7-day values were significantly greater than those for the control substrate.

3.3. Cell Morphology. When hDPSCs were cultured on the surfaces modified with different chemistries, their morphologies became different. On both days 1 and 7 (Figures 3A and 4A), the morphologies of the hDPSCs on the control surface was adherent, spindle-shaped, and elongated fibroblast-like in appearance. On day 7, the densities of the cells were elevated on the control surface, and the cells were oriented. Meanwhile, the cells grown on the –NH₂ surface became flattened and many of them displayed the typical osteoblast-like morphology and appeared to be multilayered. After analyzing the cell areas (Figure 4B) and the number of branching (Figure 4C), the results indicated that the hDPSCs cultured on the –NH₂ surface had larger cell areas and more branching than did hDPSCs on other substrates. The cells seeded on the –OH and –CH₃ surfaces displayed elongated shapes and the cells formed clusters in certain areas on the surfaces on day 1. By day 7, there were increases in cell coverage on both –OH and –CH₃ surfaces, but the cells appeared in round shapes on the –CH₃ surface and elongated shapes on the –OH surface. Most of the hDPSCs cultured on the –COOH surface appeared to be rounded on both days 1 and 7. On the basis of the fact that the hDPSCs became overly confluent in most regions on day 7, the determination of the single cell outlines was difficult so that quantification was not performed.

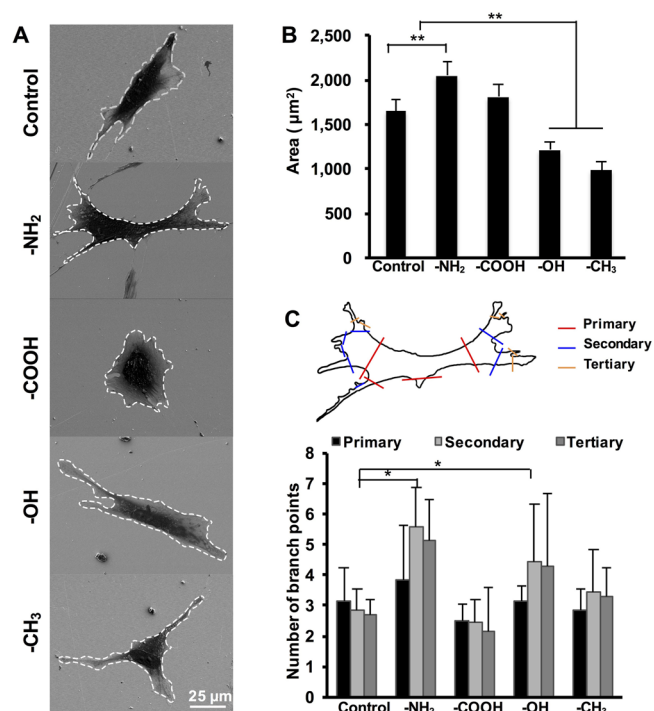


Figure 4. (A) SEM images of hDPSCs morphology cultured on surfaces with different chemical groups for 24 h. Scale bar = 25 µm. Cell morphology were quantified for (B) area and (C) number of primary, secondary, and tertiary branch points for hDPSCs cultured on different chemically modified surfaces ($n = 50$). * $P < 0.05$, ** $P < 0.01$.

3.4. Cytoskeleton and Cell Adhesion. The cell adhesion and cytoskeletal formation on the different surfaces were further detected, with focal adhesion points (FAPs) of the hDPSCs stained by using vinculin, F-actin used to label the cytoskeletal arrangement, and counterstain of nuclei using DAPI (Figure 5). From the fluorescence micrographs after 24 h of culture on the surfaces, the density of FAPs was measured. Among all the surfaces, the cells cultured on the –NH₂ surface showed the highest level of FAPs (Figure 5B). The image clearly showed that the FAPs were located within the plasma and mainly ends of the stress fibers (Figure 5B, arrow). Meanwhile, the cells cultured on the –NH₂ surface exhibited a clear cytoskeleton structure and clear evidence of stress fiber formation. The cytoskeleton formations of the hDPSCs cultured on the –COOH (Figure 5C), –OH (Figure 5D), –CH₃ (Figure 5E), and control (Figure 5A) surfaces were comparable to that observed on the –NH₂-modified substrate at 24 h, indicating that the stress fibers of viable cells on each surface could be well-formed. However, the cell adhesion revealed by FAPs suggested that the cells in contact with the –CH₃ surface displayed a significantly lower level of FAP density among all the test groups (Figure 5F), where immunostaining of vinculin could be barely detected in the hDPSCs cultured on the surface. The influences of the –COOH and the –OH surfaces toward cell adhesion were similar to those of the control group.

3.5. Influence of Chemical Modification on Osteogenic/Odontogenic Differentiation of hDPSCs. To assess the effect of different chemical groups on guiding hDPSC differentiation into the odonto/osteogenic lineage, we measured the mRNA levels of ALP, Runx2, DSPP, and DMP-1 (Figure 6A) and ALP activity (Figure 6B) after 7 days of

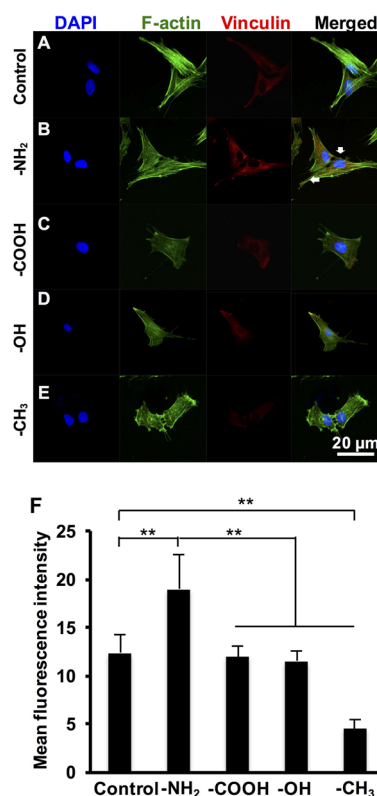


Figure 5. Confocal laser scanning microscopy images of cytoskeleton demonstrating cell adhesion and cytoskeletal formation of hDPSCs cultured on various surfaces after 24 h of culture. Immunofluorescence staining of F-actin (green), DAPI nuclear (Blue), vinculin (red), and merged images. Scale bar = 20 μm . (A) Control surface, (B) $-\text{NH}_2$ surface, (C) $-\text{COOH}$ surface, (D) $-\text{OH}$ surface, and (E) $-\text{CH}_3$ surface. (F) Mean fluorescence intensity of vinculin of hDPSCs seeded on different surfaces were quantified ($n = 50$). * $P < 0.05$, ** $P < 0.01$.

culture in the growth medium without any additional osteo/odontogenic differentiation-stimulating agents. Furthermore, Western blot (Figure 6C) and ARS staining (Figure 6D) were also performed to validate the osteogenic differentiation of hDPSCs on surfaces with various functional groups on 7 and 21 days of osteogenic induction, respectively.

The mRNA expression levels for Runx2, ALP, DSPP, and DMP-1 were compared among all the modified surfaces. The control group was set for the mRNA expression baselines (relative expression values at 100%). As indicated by the results, there was a significant increase of the four genes on the $-\text{NH}_2$ substrate at 7 days compared with those in the control group. Both DSPP and DMP-1 are hallmarks of odontoblastic differentiation.⁴¹ DSPP, expressed by odontoblastic cells and known as an odontoblast-specific marker,⁴² demonstrated a 1.87-fold increase for the cells cultured on the $-\text{NH}_2$ surface compared to those on the control substrate. Meanwhile, DMP-1, one of the noncollagenous extracellular matrix proteins, a key marker for odontoblasts,⁴³ displayed an increase of 3.16 times for cells on the $-\text{NH}_2$ -modified surface. Both DSPP and DMP-1 expression levels for the cells on the $-\text{NH}_2$ surface were higher than all the other experimental groups as well. Furthermore, two other important osteogenic markers, Runx2, which is an early stage osteo/odontogenesis-related gene,⁴⁴ and ALP, which is important for ECM mineralization,⁴⁵ were also evaluated. Both of them showed significant increases for cells grown on the $-\text{NH}_2$ surface. On the other hand, the

mRNA levels of Runx2, ALP, DSPP, and DMP-1 were not significantly and consistently affected by the $-\text{COOH}$, $-\text{OH}$, and $-\text{CH}_3$ surfaces at 7 days, when compared to control surface. Similarly, the ALP activity of the hDPSCs was significantly higher on the $-\text{NH}_2$ surface compared with those on all the other groups.

After the hDPSCs were cultured under the induction of osteogenesis on surfaces with various chemical groups for 7 days, we extracted the protein from seeded hDPSCs on all the modified surfaces and evaluated the odonto/osteogenic-related gene expression on protein level by using Western blot (Figure 6C). The results were consistent with those obtained from RT-PCR and ALP activity analysis, where the expression of protein levels for Runx-2, ALP, DSPP, and DMP-1 were all elevated on the $-\text{NH}_2$ surfaces compared with other groups. Furthermore, ARS staining for hDPSCs under osteogenesis induction for 21 days (Figure 6D) also showed that the mineral deposition by the hDPSCs on $-\text{NH}_2$ surfaces were significantly higher than all the other groups. These data indicated that $-\text{NH}_2$ could potentially promote the differentiation of hDPSCs toward the odonto/osteogenic lineage.

4. DISCUSSION

In this study, the modified Ti surface was made by coating with Au followed by inducing the formation of SAMs of alkanethiols to create well-defined surfaces presenting a range of chemical moieties with distinct characteristics.^{33–37} Using this model system, the impact of surface chemistry on the biological behaviors of hDPSCs as well as their osteo/odontogenic differentiation was investigated, which may expand our knowledge in future surface design of implants or other applications. The results demonstrated that the $-\text{NH}_2$ -modified surface could better support cell proliferation, enhance the formation of focal cell adhesion, and influence the osteo/odontogenic differentiation of the hDPSCs compared to other surfaces.

Previous studies have indicated that nanoscale surface modifications have the ability to modulate the biological activity of cells.^{46–48} Thus, to achieve a convincing chemical modification, we used the electron beam evaporation technique to create Au films with a thickness of 40 nm, which were proven to be flat for the subsequent modification with chemical functional groups. The functional groups were successfully generated on the surfaces through self-assembly and they had similar densities/nanoscale topographic features according to analyses in our previous studies^{34–36} as well as XPS measurements (Figure S2, Tables S1 and S2). Therefore, the cell behaviors should not have been affected by the nanoscale features,^{46–48} if any, on our surfaces.

The hydrophilicity of chemical surface was observed to affect the viability and morphology of the hDPSCs. It is well-known that the hydrophilicity is a key factor of surface modification in directing cell and tissue behaviors.^{49,50} Further influence of surface chemistry and its hydrophilicity on cell morphology have been also demonstrated by previous studies.^{9–12} In our study, the hDPSCs seemed to specifically prefer to spread out on the hydrophilic $-\text{NH}_2$ surface with a high-branching, elongated morphology. The proliferation rate of the cells on the $-\text{NH}_2$ -modified surface was significantly higher than those on all the other test groups. Although the cells could also attach to the most hydrophobic $-\text{CH}_3$ surface, they appeared in a smaller, more compact, and rounded morphology. Moreover, based on F-actin staining images, among all the experimental

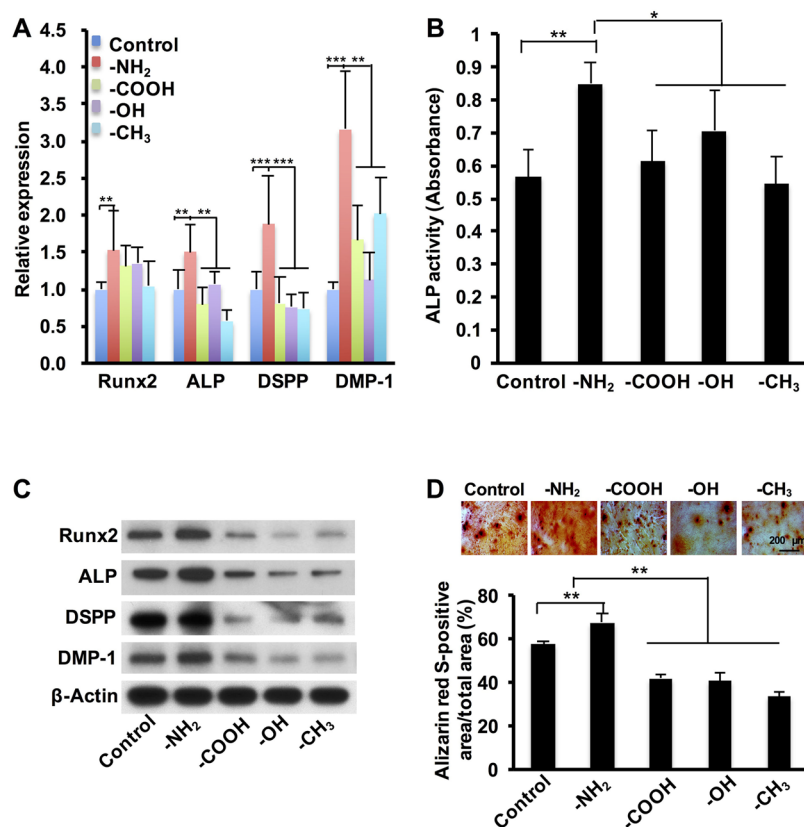


Figure 6. Chemical functional groups altered hDPSCs osteo/odontogenic differentiation through the detection of (A) osteo/odontogenic-related gene expression and (B) ALP production. Both mRNA levels and ALP activity were investigated after 7 days of culture in growth medium without any osteo/odontogenic differentiation-related stimuli factors. (C) Western blot and (D) ARS staining were measured after the cells were induced in osteogenic medium for 7 and 21 days. Scale bar = 200 μm . * $P < 0.05$, ** $P < 0.01$, *** $P < 0.001$.

groups, the cells cultured on the $-\text{NH}_2$ surface exhibited a well-defined cytoskeleton structure and clear evidence of stress fiber formation. It has been demonstrated in previous study that thick and clear stress fiber formation could facilitate downstream cellular activities and induce differentiation of MSCs.⁵¹ Indeed, the hDPSCs cultured on the $-\text{OH}$, $-\text{COOH}$, and $-\text{CH}_3$ surfaces maintained the MSCs phenotype as those cultured on control surfaces. Cell viability data further proved that the $-\text{OH}$ and $-\text{COOH}$ surfaces maintained the cell viability, while the cells grown on the $-\text{CH}_3$ surface displayed the lowest proliferation rate compared with the other substrates, indicating the effect of hydrophilicity. The morphology, FAP density, orientation, and odonto/osteogenic related gene and protein expressions of hDPSCs cultured on the $-\text{CH}_3$, $-\text{OH}$, $-\text{COOH}$, and control surfaces seemed to exhibit no apparent changes.

Nevertheless, the hDPSCs cultured on the $-\text{NH}_2$ surface not only displayed larger spreading area with multiple extending pseudopodia, the focal adhesion density was also the highest among all the groups. In contrast, the cells in contact with the $-\text{CH}_3$ -modified surface exhibited a rounded morphology as well as the lowest FAP density. As Barcabac et al. suggested, rounded cells appeared to be less adherent and displayed a thin cytoskeleton conformation compared to flatter cells.⁵² This result might be attributed to the different composition of surface chemistry, surface free energy, and/or hydrophobicity as previously demonstrated.^{49,50} Furthermore, on the basis of previous studies on the nonspecific protein and detergent adsorptions to SAMs of alkanethiolates on Au,⁵³ the correlation

between the wettability of the SAMs and the adsorbed protein size was demonstrated. Proteins with smaller and larger sizes among those tested were adsorbed on the least wettable surfaces. Therefore, in our study, both the adhesion and proliferation of the hDPSCs cultured in contact with the hydrophilic surfaces ($-\text{OH}$, $-\text{COOH}$) and moderately wettable surface ($-\text{NH}_2$) were promoted in comparison to the hydrophobic surface ($-\text{CH}_3$). This effect might have occurred because surface proteins exhibited less organized secondary structures on hydrophobic surfaces than hydrophilic ones.⁵⁴ Similarly, Barrias et al. examined the interplay between stem cell adhesion and the adsorption of adhesive proteins on various $-\text{OH}/-\text{CH}_3$ SAMs with different wettabilities.⁵⁵ They found that $-\text{OH}$ SAMs better sustained the cell-binding activity of proteins and stem cell adhesion as compared with the hydrophobic $-\text{CH}_3$ SAMs. These results were consistent with our findings and may provide us a method to illustrate the interaction between surface chemistry and cell attachment.

Having a good biocompatibility is essential for implants, and the ability to actively induce cells toward odonto/osteogenic differentiation is also desired. Our study showed that the hDPSCs cultured on the $-\text{NH}_2$ surface exhibited a highly branching, well-spread, elongated morphology, maintaining a statistically significantly higher density of FAPs by 24 h than the cells on all other surfaces. By day 7, the hDPSCs reached a confluent monolayer and well-orientated spreading. It is known that cell adhesion and morphology can mediate their biological behaviors, such as metabolism, signal transduction, and fate commitment.^{9,56–58} In our study, the changes in the

morphology and increased FAP density of the hDPSCs resulted in an increase in ALP activity, which represents an early marker of odonto/osteogenic differentiation. At the mRNA level, the specific osteo/odontogenesis-related genes were significantly elevated after the culture of hDPSCs on the $-NH_2$ -modified substrate compared to all the other substrates. Furthermore, Western blot and ARS staining results also supported these findings. Collectively, it seems that the hDPSCs preferred to attach to the $-NH_2$ -modified surface and could form a highly branching “osteoblast-like” morphology, which could have pushed them toward an odonto/osteogenesis pathway instead of maintaining the mesenchymal phenotype or differentiating into other cell types. Better surface hydrophilicity is known to promote early osseointegration of implants by inducing better early cellular response of bone-forming cells via the increased adsorption of cell adhesion proteins.^{46,59} Thus, the $-NH_2$ surface possessing a proper wettability is anticipated to be beneficial for achieving osteogenesis as compared with the most hydrophobic surface ($-CH_3$) or the most hydrophilic surface ($-OH$).

5. CONCLUSIONS

By utilizing alkanethiol-based SAM technique, a range of well-defined surfaces with different chemistries were successfully created, terminated with $-NH_2$, $-OH$, $-COOH$, and $-CH_3$ functional groups. Their distinct surface hydrophilicity and chemical characteristics contributed to direct the biological behaviors of hDPSCs. In this study, the $-NH_2$ surface was found to not only sustain the viability of the hDPSCs, but to also direct the cells to commit to the specific odonto/osteogenic lineage potentially through enhanced cell focal adhesion, cytoskeleton structure, and cell morphology changes. The hDPSCs cultured on the control, $-COOH$, $-OH$, and $-CH_3$ surfaces preferred to maintain the mesenchymal phenotype. These findings suggested that, a simple chemical modification on biomaterial surfaces may be used to control the complicated cell-matrix interactions and cell functions. The findings have provided us with a strategy for improving the biocompatibility and osseointegration of dental implant materials, and may be further expanded for use in bone graft or plastic surgery. As we realize the limitation of the current study, more biological behaviors of hDPSCs such as viability, phenotype maintenance, and multiple-lineage determination are currently under exploration and will be reported in future publications. Furthermore, the underlying mechanisms of the different surface chemistries on the behaviors of the hDPSCs still require more systematic investigations and possibly in vivo validation.

■ ASSOCIATED CONTENT

Supporting Information

The Supporting Information is available free of charge on the ACS Publications website at DOI: [10.1021/acsbomaterials.7b00274](https://doi.org/10.1021/acsbomaterials.7b00274).

Figures S1 and S2, Tables S1 and S2 (PDF)

■ AUTHOR INFORMATION

Corresponding Authors

*E-mail: yszhang@research.bwh.harvard.edu. Tel.: +1-617-768-8581.

*E-mail: fyang@iccas.ac.cn. Tel.: +86-10-62565822. Fax: +86-10-62581241.

*E-mail: yanhengzhou@vip.163.com. Tel.: +86-10-82195728. Fax: +86-10-82195536.

ORCID

De-Cheng Wu: 0000-0002-5276-8607

Yu Shrike Zhang: 0000-0001-8642-133X

Author Contributions

T.-T.Y. conducted the experiments, designed the experiments, and drafted the manuscript; Y.S.Z., F.Y., and Y.-H.Z. designed the experiment and critically revised the manuscript; F.-Z.C., Q.-Y.M., X.-X.K., J.W., and D.-C.W. contributed to data arrangement and organized the manuscript; J.Z., R.-L.Y., Y.L. helped with data analysis and critically revised the manuscript. All authors read and gave approval to the final manuscript.

Notes

The authors declare no competing financial interest.

■ ACKNOWLEDGMENTS

This work was supported by the International Science & Technology Cooperation Program of China 2015DFB30040 (Y.Z.), the National Natural Science Foundations of China 81300897 (X.K.), 81571815 (Y.L.), 81671015 (X.W.), and 81470717 (Y.Z.), and the Beijing Municipal Natural Science Foundation 7152156 (Y.L.). We give our sincere thanks to Dr. Jianxun Ding from Changchun Institute of Applied Chemistry, Chinese Academy of Science, for reviewing and editing the manuscript.

■ REFERENCES

- (1) Annunziata, M.; Guida, L. The effect of titanium surface modifications on dental implant osseointegration. *Front. Oral Biol.* **2015**, *17*, 62–77.
- (2) Montebugnoli, L.; Venturi, M.; Cervellati, F.; Servidio, D.; Vocale, C.; Pagan, F.; Landini, M. P.; Magnani, G.; Sambri, V. Peri-implant response and microflora in organ transplant patients 1 year after prosthetic loading: a prospective controlled study. *Clin. Implant Dent. Relat. Res.* **2015**, *17*, 972–982.
- (3) Marco, F.; Milena, F.; Gianluca, G.; Vittoria, O. Peri-implant osteogenesis in health and osteoporosis. *Micron* **2005**, *36*, 630–644.
- (4) Testori, T.; Clauser, C.; Deflorian, M.; Capelli, M.; Zuffetti, F.; Fabbro, M. D. A retrospective analysis of the effectiveness of the longevity protocol for assessing the risk of implant failure. *Clin. Implant Dent. Relat. Res.* **2016**, *18*, 1113–1118.
- (5) Esposito, M.; Ardebili, Y.; Worthington, H. V. Interventions for replacing missing teeth: different types of dental implants. *Cochrane Database Syst. Rev.* **2014**, *7*, CD003815.
- (6) Li, P. J.; de Groot, K. A calcium phosphate formation within sol-gel-prepared titania in vitro and in vivo. *J. Biomed. Mater. Res.* **1993**, *27*, 1495–1500.
- (7) Campbell, A. A.; Song, L.; Li, X. S.; Nelson, B. J.; Bottoni, C.; Brooks, D. E.; DeJong, E. S. Development, characterization, and antimicrobial efficacy of hydroxyapatite-chlorhexidine coatings produced by surface-induced mineralization. *J. Biomed. Mater. Res.* **2000**, *53*, 400–407.
- (8) Benoit, D. S.; Schwartz, M. P.; Durney, A. R.; Anseth, K. S. Small molecule functional groups for controlled differentiation of hydrogel-encapsulated human mesenchymal stem cells. *Nat. Mater.* **2008**, *7*, 816–823.
- (9) Keselowsky, B. G.; Collard, D. M.; Garcia, A. J. Surface chemistry modulates focal adhesion composition and signaling through changes in integrin binding. *Biomaterials* **2004**, *25*, 5947–5954.
- (10) Curran, J. M.; Chen, R.; Hunt, J. A. Controlling the phenotype and function of mesenchymal stem cells in vitro by adhesion to silane modified clean glass surfaces. *Biomaterials* **2005**, *26*, 7057–7067.

- (11) Curran, J. M.; Chen, R.; Hunt, J. A. The guidance of human mesenchymal stem cell differentiation in vitro by controlled modifications to the cell substrate. *Biomaterials* **2006**, *27*, 4783–4793.
- (12) Ren, Y. J.; Zhang, H.; Huang, H.; Wang, X. M.; Zhou, Z. Y.; Cui, F. Z.; An, Y. H. In vitro behavior of neural stem cells in response to different chemical functional groups. *Biomaterials* **2009**, *30*, 1036–1044.
- (13) Bai, B.; He, J.; Li, Y. S.; Wang, X. M.; Ai, H. J.; Cui, F. Z. Activation of the ERK1/2 signaling pathway during the osteogenic differentiation of mesenchymal stem cells cultured on substrates modified with various chemical groups. *BioMed Res. Int.* **2013**, *2013*, 361906.
- (14) Hynes, R. O. Integrins: bidirectional, allosteric signaling machines. *Cell* **2002**, *110*, 673–687.
- (15) Ventre, M.; Netti, P. A. Engineering cell instructive materials to control cell fate and functions through material cues and surface patterning. *ACS Appl. Mater. Interfaces* **2016**, *8*, 14896–14908.
- (16) McBeath, R.; Pirone, D. M.; Nelson, C. M.; Bhadriraju, K.; Chen, C. S. Cell shape, cytoskeletal tension, and RhoA regulate stem cell lineage commitment. *Dev. Cell* **2004**, *6*, 483–495.
- (17) Allen, L. T.; Fox, E. J.; Blute, I.; Kelly, Z. D.; Rochev, Y.; Keenan, A. K.; Dawson, K. A.; Gallagher, W. M. Interaction of soft condensed materials with living cells: phenotype/transcriptome correlations for the hydrophobic effect. *Proc. Natl. Acad. Sci. U. S. A.* **2003**, *100*, 6331–6336.
- (18) Wang, Y.; Yao, S.; Meng, Q.; Yu, X.; Wang, X.; Cui, F. Gene expression profiling and mechanism study of neural stem cells response to surface chemistry. *Regen. Biomater.* **2014**, *1*, 37–47.
- (19) Huang, G. T.; Gronthos, S.; Shi, S. Mesenchymal stem cells derived from dental tissues vs. those from other sources: their biology and role in regenerative medicine. *J. Dent. Res.* **2009**, *88*, 792–806.
- (20) Gronthos, S.; Mankani, M.; Brahimi, J.; Robey, P. G.; Shi, S. Postnatal human dental pulp stem cells (DPSCs) in vitro and in vivo. *Proc. Natl. Acad. Sci. U. S. A.* **2000**, *97*, 13625–13630.
- (21) Gronthos, S.; Brahimi, J.; Li, W.; Fisher, L. W.; Cherman, N.; Boyde, A.; DenBesten, P.; Robey, P. G.; Shi, S. Stem cell properties of human dental pulp stem cells. *J. Dent. Res.* **2002**, *81*, 531–535.
- (22) Alge, D. L.; Zhou, D.; Adams, L. L.; Wyss, B. K.; Shadday, M. D.; Woods, E. J.; Gabriel Chu, T. M.; Goebel, W. S. Donor-matched comparison of dental pulp stem cells and bone marrow-derived mesenchymal stem cells in a rat model. *J. Tissue Eng. Regen. Med.* **2010**, *4*, 73–81.
- (23) Yasui, T.; Mabuchi, Y.; Toriumi, H.; Ebine, T.; Niibe, K.; Houlihan, D. D.; Morikawa, S.; Onizawa, K.; Kawana, H.; Akazawa, C.; Suzuki, N.; Nakagawa, T.; Okano, H.; Matsuzaki, Y. Purified human dental pulp stem cells promote osteogenic regeneration. *J. Dent. Res.* **2016**, *95*, 206–214.
- (24) Kuo, T. F.; Lee, S. Y.; Wu, H. D.; Poma, M.; Wu, Y. W.; Yang, J. C. An in vivo swine study for xeno-grafts of calcium sulfate-based bone grafts with human dental pulp stem cells (hDPSCs). *Mater. Sci. Eng., C* **2015**, *50*, 19–23.
- (25) Kwon, D. Y.; Kwon, J. S.; Park, S. H.; Park, J. H.; Jang, S. H.; Yin, X. Y.; Yun, J. H.; Kim, J. H.; Min, B. H.; Lee, J. H.; Kim, W. D.; Kim, M. S. A computer-designed scaffold for bone regeneration within cranial defect using human dental pulp stem cells. *Sci. Rep.* **2015**, *5*, 12721.
- (26) Mangano, C.; De Rosa, A.; Desiderio, V.; d'Aquino, R.; Piattelli, A.; De Francesco, F.; Tirino, V.; Mangano, F.; Papaccio, G. The osteoblastic differentiation of dental pulp stem cells and bone formation on different titanium surface textures. *Biomaterials* **2010**, *31*, 3543–3551.
- (27) Li, R.; Guo, W. H.; Yang, B.; Guo, L. J.; Sheng, L.; Chen, G.; Li, Y.; Zou, Q.; Xie, D.; An, X. X.; Chen, Y. L.; Tian, W. D. Human treated dentin matrix as a natural scaffold for complete human dentin tissue regeneration. *Biomaterials* **2011**, *32*, 4525–4538.
- (28) Jiao, L.; Xie, L.; Yang, B.; Yu, M.; Jiang, Z. T.; Feng, L.; Guo, W. H.; Tian, W. D. Cryopreserved dentin matrix as a scaffold material for dentin-pulp tissue regeneration. *Biomaterials* **2014**, *35*, 4929–4939.
- (29) Galler, K. M.; Widbiller, M.; Buchalla, W.; Eidt, A.; Hiller, H. A.; Hoffer, P. C.; Schmalz, G. EDTA conditioning of dentine promotes adhesion, migration and differentiation of dental pulp stem cells. *Int. Endod. J.* **2016**, *49*, 581–590.
- (30) Petridis, X.; Diamanti, E.; Trigas, G. C.; Kalyvas, D.; Kitraki, E. Bone regeneration in critical-size calvarial defects using human dental pulp cells in an extracellular matrix-based scaffold. *J. Craniomaxillofac. Surg.* **2015**, *43*, 483–490.
- (31) Volponi, A. A.; Gentleman, E.; Fatscher, R.; Pang, Y. W. Y.; Gentleman, M. M.; Sharpe, P. T. Composition of mineral produced by dental mesenchymal stem cells. *J. Dent. Res.* **2015**, *94*, 1568–1574.
- (32) Fu, Y.; Liu, S.; Cui, S. J.; Kou, X. X.; Wang, X. D.; Liu, X. M.; Sun, Y.; Wang, G. N.; Liu, Y.; Zhou, Y. H. Surface chemistry of nanoscale mineralized collagen regulates periodontal ligament stem cell fate. *ACS Appl. Mater. Interfaces* **2016**, *8*, 15958–15966.
- (33) Bain, C. D.; Whitesides, G. M. Molecular-level control over surface order in self-assembled monolayer films of thiols on gold. *Science* **1988**, *240*, 62–63.
- (34) Liu, Z. X.; Wang, X. M.; Wang, Q.; Shen, X. C.; Liang, H.; Cui, F. Z. Evolution of calcium phosphate crystallization on three functional group surfaces with the same surface density. *CrystEngComm* **2012**, *14*, 6695–6701.
- (35) Deng, H.; Wang, X. M.; Du, C.; Shen, X. C.; Cui, F. Z. Combined effect of ion concentration and functional groups on surface chemistry modulated CaCO₃ crystallization. *CrystEngComm* **2012**, *14*, 6647–6653.
- (36) Hao, L. J.; Fu, X. L.; Li, T. J.; Zhao, N. R.; Shi, X. T.; Cui, F. Z.; Du, C.; Wang, Y. J. Surface chemistry from wettability and charge for the control of mesenchymal stem cell fate through self-assembled monolayers. *Colloids Surf., B* **2016**, *148*, 549–556.
- (37) Scotchford, C. A.; Cooper, E.; Leggett, G. J.; Downes, S. Growth of human osteoblast-like cells on alkanethiol on gold self-assembled monolayers: the effect of surface chemistry. *J. Biomed. Mater. Res.* **1998**, *41*, 431–442.
- (38) Kumar, G.; Tison, C. K.; Chatterjee, K.; Pine, P. S.; McDaniel, J. H.; Salit, M. L.; Young, M. F.; Simon, C. G., Jr. The determination of stem cell fate by 3D scaffold structures through the control of cell shape. *Biomaterials* **2011**, *32*, 9188–9196.
- (39) Folkman, J.; Moscona, A. Role of cell shape in growth control. *Nature* **1978**, *273*, 345–349.
- (40) Kou, X. X.; Wu, Y. W.; Ding, Y.; Hao, T.; Bi, R. Y.; Gan, Y. H.; Ma, X. 17β-estradiol aggravates temporomandibular joint inflammation through the NF-κB pathway in ovariectomized rats. *Arthritis Rheum.* **2011**, *63*, 1888–1897.
- (41) Fisher, L. W.; Fedarko, N. S. Six genes expressed in bones and teeth encode the current members of the SIBLING family of proteins. *Connect. Tissue Res.* **2003**, *44*, 33–40.
- (42) Hanks, C. T.; Fang, D.; Sun, Z.; Edwards, C. A.; Butler, W. T. Dentin-specific proteins in MDPC-23 cell line. *Eur. J. Oral Sci.* **1998**, *106*, 260–266.
- (43) Narayanan, K.; Srinivas, R.; Ramachandran, A.; Hao, J.; Quinn, B.; George, A. Differentiation of embryonic mesenchymal cells to odontoblast-like cells by overexpression of dentin matrix protein 1. *Proc. Natl. Acad. Sci. U. S. A.* **2001**, *98*, 4516–4521.
- (44) Camilleri, S.; McDonald, F. Runx2 and dental development. *Eur. J. Oral Sci.* **2006**, *114*, 361–373.
- (45) Marom, R.; Shur, I.; Solomon, R.; Benayahu, D. Characterization of adhesion and differentiation markers of osteogenic marrow stromal cells. *J. Cell. Physiol.* **2005**, *202*, 41–48.
- (46) Khang, D.; Choi, J.; Im, Y. M.; Kim, Y. J.; Jang, J. H.; Kang, S. S.; Nam, T. H.; Song, J.; Park, J. W. Role of subnano-, nano- and submicron-surface features on osteoblast differentiation of bone marrow mesenchymal stem cells. *Biomaterials* **2012**, *33*, 5997–6007.
- (47) Puckett, S.; Pareta, R.; Webster, T. J. Nano rough micron patterned titanium for directing osteoblast morphology and adhesion. *Int. J. Nanomed.* **2008**, *3*, 229–241.
- (48) Sjöström, T.; Dalby, M. J.; Hart, A.; Tare, R.; Oreffo, R. O.; Su, B. Fabrication of pillar-like titania nanostructures on titanium and their

interactions with human skeletal stem cells. *Acta Biomater.* **2009**, *5*, 1433–1441.

(49) Wang, J.; Wang, X.; Yang, F.; Shen, H.; You, Y.; Wu, D. Effect of topological structures on the self-assembly behavior of supramolecular amphiphiles. *Langmuir* **2015**, *31*, 13834–13841.

(50) Bu, Y.; Zhang, L.; Liu, J.; Zhang, L.; Li, T.; Shen, H.; Wang, X.; Yang, F.; Tang, P.; Wu, D. Synthesis and properties of hemostatic and bacteria-responsive in situ hydrogels for emergency treatment in critical situations. *ACS Appl. Mater. Interfaces* **2016**, *8*, 12674–12683.

(51) Müller, P.; Langenbach, A.; Kaminski, A.; Rychly, J. Modulating the actin cytoskeleton cells. *PLoS One* **2013**, *8*, e71283.

(52) Bacabac, R. G.; Mizuno, D.; Schmidt, C. F.; MacKintosh, F. C.; Van Loon, J. J.; Klein-Nulend, J.; Smit, T. H. Round versus flat: Bone cell morphology, elasticity, and mechanosensing. *J. Biomech.* **2008**, *41*, 1590–1598.

(53) Sigal, G. B.; Mrksich, M.; Whitesides, G. M. Effect of surface wettability on the adsorption of proteins and detergents. *J. Am. Chem. Soc.* **1998**, *120*, 3464–3473.

(54) Roach, P.; Farrar, D.; Perry, C. C. Interpretation of protein adsorption: surface-induced conformational changes. *J. Am. Chem. Soc.* **2005**, *127*, 8168–8173.

(55) Barrias, C. C.; Martins, M. C.; Almeida-Porada, G.; Barbosa, M. A.; Granja, P. L. The correlation between the adsorption of adhesion of adhesive proteins and cell behavior on hydroxyl-methyl mixed self-assembled monolayers. *Biomaterials* **2009**, *30*, 307–316.

(56) Boyan, B. D.; Hummert, T. W.; Dean, D. D.; Schwartz, Z. Role of material surfaces in regulating bone and cartilage cell response. *Biomaterials* **1996**, *17*, 137–146.

(57) Ingber, D. E. Tensegrity II. How structural networks influence cellular information processing networks. *J. Cell Sci.* **2003**, *116*, 1397–1408.

(58) Córdoba, A.; Monjo, M.; Hierro-Oliva, M.; González-Martín, M. L.; Ramis, J. M. Bioinspired quercitrin nanocoatings: A fluorescence-based method for their surface quantification, and their effect on stem cell adhesion and differentiation to the osteoblastic lineage. *ACS Appl. Mater. Interfaces* **2015**, *7*, 16857–16864.

(59) Lang, N. P.; Salvi, G. E.; Huynh-Ba, G.; Ivanovski, S.; Donos, N.; Bosshardt, D. D. Early osseointegration to hydrophilic and hydrophobic implant surfaces in humans. *Clin. Oral Implants Res.* **2011**, *22*, 349–356.